Journal of Machine Engineering, 2025, Vol. 25, No.4, 75–90
ISSN 1895-7595 (Print) ISSN 2391-8071 (Online)

Received*: 20 November 2025* / Accepted: *29 November 2025* / Published online: *1 December 2025*

artificial neural networks,
finite element method,
error compensation,
train wheel set

Pawel MACIOLKA[1*]

A HYBRID MODELLING FOR MACHINING ERROR COMPENSATION IN SPECIALIZED MACHINE TOOL FOR TRAIN WHEEL SETS

The aim of this study was to develop and verify a hybrid method for modelling machining errors in a specialized machine tool used for reconditioning and profiling train wheels, combining the finite element method (FEM) with artificial neural networks (ANNs). A detailed numerical model was created, incorporating both machine tool components and the machined wheelset. This model enabled analysis of cutting-force-induced elastic deformations under realistic boundary conditions, variable system stiffness, and the specific method of supporting the wheelset in centres and on driving rollers. Results from FEM simulations were used to build a database for training an ANN capable of rapidly and accurately predicting radial and axial deformations as functions of cutting forces and related machining parameters. This allowed the development of a functional form of machining error suitable for use in numerical control (NC) systems. Testing confirmed that the ANN effectively reproduced the error magnitudes obtained from FEM simulations. Its application significantly improved prediction efficiency while keeping computational time very low. The proposed method supports indirect error compensation through real-time measurement of cutting forces and corresponding tool-path correction, representing an important step toward intelligent machining systems. Further work on refining the functional form of machining errors will focus on expanding ANN inputs to include wheelset design parameters, enhancing the model's generality and compensation capabilities.

1. INTRODUCTION

The compensation of errors in machine tools has been the subject of extensive research for several decades now. The accuracy of machining processes is strongly affected by: the structure's stiffness and its thermal displacements and the control system's dynamic response and precision. The dominant source of machining errors are the elastic deformations of the mechanical parts, thermally induced displacements and the geometrical inaccuracies of the

[1] Faculty of Mechanical Engineering, Wroclaw University of Science and Technology, Poland
[*] E-mail: pawel.maciolka@pwr.edu.pl
https://doi.org/10.36897/jme/214903

feed drives. Various methods of modelling, monitoring and compensating the errors have been developed over years.

Sensor-based methods focus on process measurement and control in real time by means of various sensors recording cutting forces, vibrations, temperatures and tool displacements, the signals of which are the basis for introducing corrections. Shokrani et al. [1] presented a survey of various sensors used for measuring and monitoring in-process and on-machine parameters, such as cutting forces, vibrations, tool wear and surface integrity. They also examined data transmission and communication methods and power supply options for systems integrated with sensors.

Parametric methods use machine and NC program internal data, such as feed rate, spindle position, cutting forces and driving torque, to predict and compensate errors. The offline compensation method is based on error forecasting models, which enables one to adjust a machining program before starting machining. Wu et al. [2] introduced an iterative strategy for compensation through cutter location source file (CLSF) modification based on on-machine measurements (OMM) and a thin-walled parts stiffness FE (finite element) model in order to predict deformations during machining.

Hybrid methods combine the attributes of the two approaches – they integrate sensor measurement data or machine tool internal parameters with model-based prediction. Li et al. [3] developed a real-time deformation model applicable to both thin-walled parts and tools, demonstrating that real-time force measurements combined with parametric corrections can effectively reduce dimensional errors. This solution was also verified for one-dimensional cases and it was planned to be implemented in two- or three-dimensional compensation strategies and devices. Ge et al. [4] extended this concept onto three axes through an on-machine measurement (OMM) system and an error compensation algorithm using external machine zero point shift (EMZPS) functions integrated with a Fanuc NC system.

Recently Naumann et al. [5] proposed a hybrid compensation strategy for a five-axis machining centre DMU 80 eVo, combining deformation detection by means of integrated sensors inside the machine tool with compensation based on deformation characteristics, and demonstrated good adaptation to the selected table position. The research aims at correction for different table locations in the workspace. Geng et al. [6] reviewed the different geometric error calibration methods and proposed a unified calibration procedure for ultra-precision machine tools (UPMT).

Even though there are numerous studies on machine tool error compensation, only a few of them deal with the machine tool-workpiece interaction as a coupled system. Denkena et al. [7] presented a combined machine tool structure-workpiece mechanical model for estimating total deformation on the basis of cutting force simulations. Brecher et al. [8] highlighted the importance of the use of cutting force measurements as reference data for the compensation of tooth path deflections during milling. Piorkowski et al. [9] showed that a statistical analysis of machined surfaces can be helpful in the quantitative determination of process stability, but it lacks prediction capabilities for complex real-time compensation.

The above research clearly indicates that accurate and efficient error forecasting models are indispensable, particularly in the case of specialized and large-size machine tools in which the system’s stiffness and the workpiece’s geometry significantly affect machining precision. The combination of FEM and the ANN method is a forward-looking approach combining

FEM's high fidelity of mapping physical phenomena with the ANN method's high computing speed and effectiveness. The FE model supplies detailed information on the distribution of deformations in boundary conditions close to the real ones, while ANNs enable the fast approximation of complex nonlinear relations, such as the ones between temperature or cutting forces and the resulting displacements.

Until now the machining errors of train wheel sets have not been widely investigated. In the literature on the subject one can find numerous studies dealing with error compensation in the particular units of conventional machine tools and also studies covering complex models of whole general-purpose machine tools. Lei et al. [10] presented a compensation method owing to which high positioning accuracy of linear feed drives was achieved. One can familiarize oneself with the designs of detailed models of major machine tool units in a paper by Kowal et al. [11] which describes the modelling of prestressed ball screws in different operating conditions. Jedrzejewski et al. [12] present their own elaborate system for modelling machine tool operating conditions. All the above papers cover the feed drive and the whole structure of commonly produced general-purpose machine tools subjected to force and thermal loads, but most of them do not cover the workpiece. The scope of this work includes modelling of machining errors resulting from elastic deformations occurring during the process of cutting railway wheels on a specialized machine tool. Permissible deviations in dimensions, shape, and measurement methods are defined by instructions from wheel set users, developed based on standards. For example, information on train wheel profile can be found in the PN-EN 13715:2020-12 standard [13].

The proposed here hybrid approach integrates computational methods based on FEM simulations and ANNs with measurement data from sensors whereby effective machining error prediction and compensation is ensured for the specialized machine tool used for the reconditioning and profiling of train wheel sets. The methodology involves the following three main stages:

(1) the numerical modelling of the machine-workpiece system for the purpose of simulating elastic deformations under variable cutting forces,

(2) the training and validation of an ANN prediction model,

(3) the implementation of the functional error model in real-time compensation in an NC system.

2. FE WHEEL SET MODEL

In stage 1 the machine tool's behaviour was determined on the basis of a detailed FE model making it possible to map and analyse the actual machine tool behaviour in various operating conditions.

The FE model covered both the machine tool and the wheel set whereby the disturbances and the values of the errors affecting machining quality could be precisely identified.

The detailed FE model took into account (among other things):

- the heat sources acting on the machine tool,
- the heat exchange between the machine tool's components and the environment,
- the heat transfer between the machine tool's units,

- the initial temperature,
- the loads generated by the clamping and cutting forces,
- the machine tool's design and the arrangement of its units in the workspace.

In the case of machine tools for train wheels, the identification of errors caused by the elastic deformations of the wheel set under the cutting forces is of key importance. Due to the wheel set's high compliance and dimensions the above has a significant bearing on machining accuracy. For this reason, modelling and simulations which took into account the way of wheel set clamping with centres and driving rollers (Fig. 1) were carried out. The wheel set supported in the centres is connected with the rest of the machine tool structure via aligning sleeves.

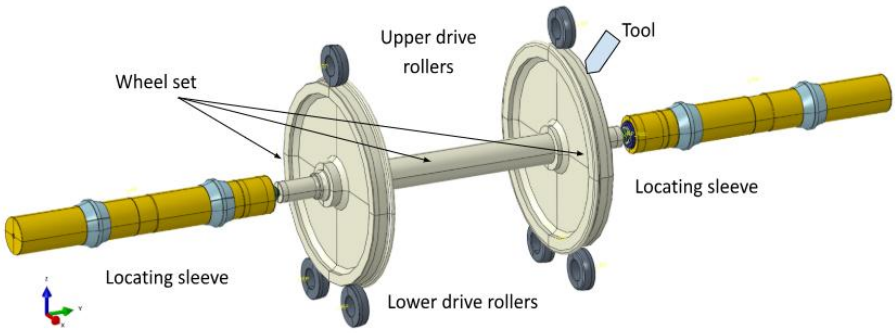

Fig. 1. Wheel set model with places of force interactions stemming from aligning and clamping system (sleeves with centers inside) and friction drives (top rollers and bottom rollers)

The set of forces and their interactions are shown in Fig. 2. Moreover, in order to build a detailed model (Fig. 2) it was necessary to select:

- the type of finite elements to be used,
- space division density with regard to both workpiece geometry and finite element grid quality, and
- time division density.

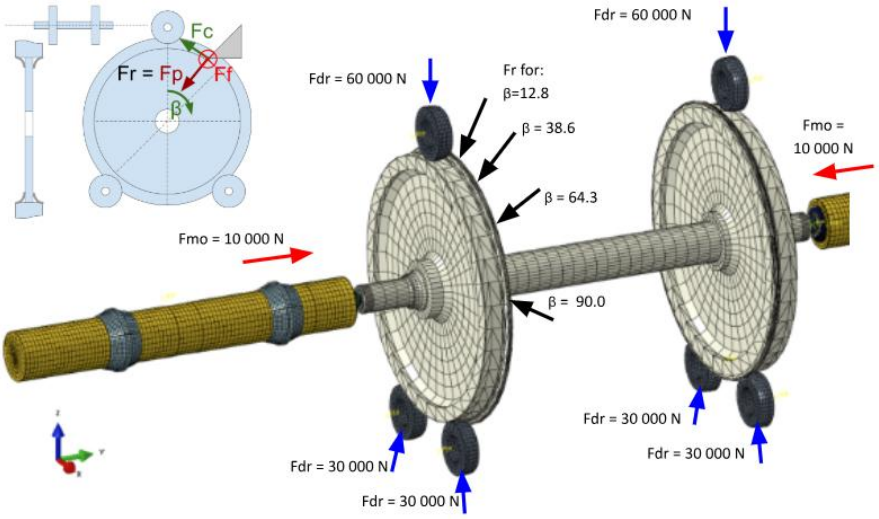

Fig. 2. Wheel set FE model and boundary conditions: F_{mo} – clamping force, F_{dr} – roller pressure force, F_r – radial force acting at selected angles β on the circumference of the wheel, $F_p = Fr$ is cutting resistance force, F_c – cutting force and F_f – feed force (axial force)

In order to ensure high computing accuracy a densified mesh in places of force interactions was prepared and a way of modelling the wheel set aligning and clamping centre bearings (Fig. 3) was developed.

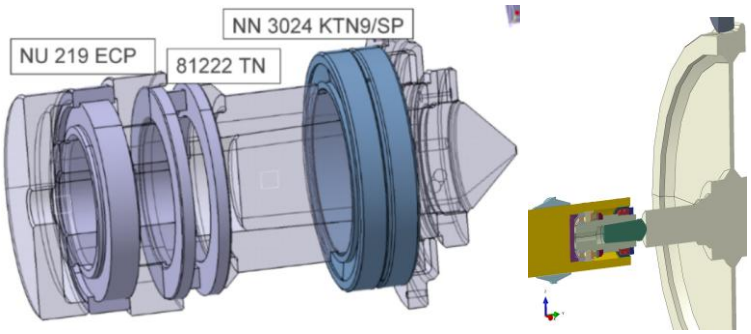

Fig. 3. Centre with bearings

Considering computational efficiency, the mapping of the geometry of the bearings' rolling elements was skipped and the geometry was replaced with that of an appropriate ring element. The actual stiffness of the bearings in the simplified centre model (Fig. 3) was taken into account by:

1. introducing an equivalent E-modulus for the simplified ball bearing model (Fig. 4b) on the basis of computations of the bearing precisely modelled using the FE model (Fig. 4a).

a) b)

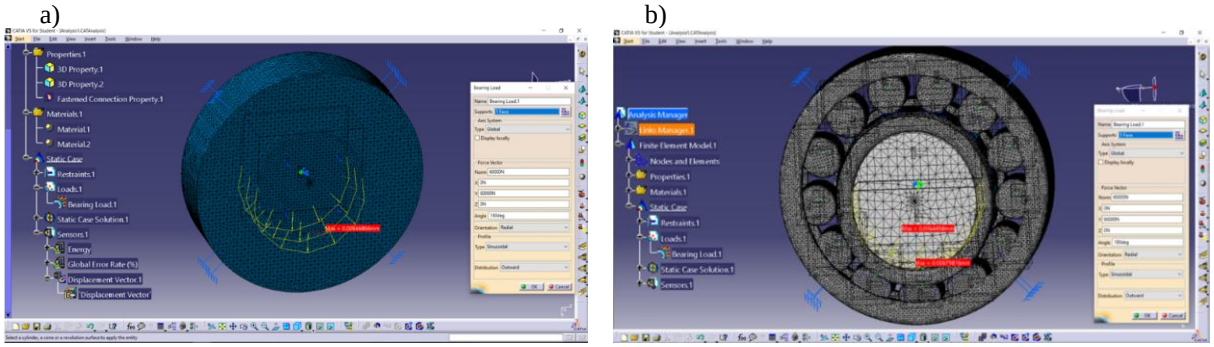

Fig. 4. Structures with identical center displacements for exemplary loads: a) equivalent structure, b) real structure

2. Introducing the bearing's catalogue stiffness in the contact layer between the bearing and its retainer (Fig. 5) in conformance with the 6.14 Abaqus Standard system's capabilities.

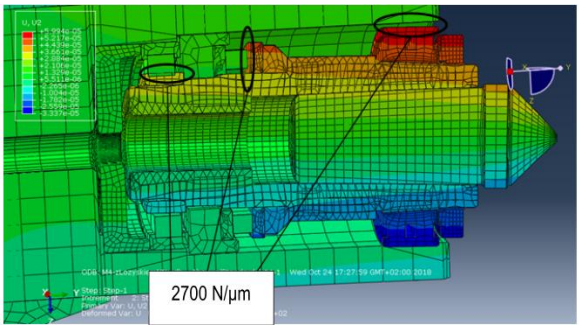

Fig. 5. Centre structure with contact layers having catalogue bearing stiffness

It follows from the above ways of bearing modelling that the introduction of the catalogue bearing stiffness into the contact layer between the bearing and its retainer is the simplest solution most close to the actual behaviour of the wheel set structure (2700 N/μm in Fig. 5). Shear deformations between the centre and the wheel's centre hole were taken into account in the model, leaving out contact deformations in this area as indicated by study [14] where it was shown that deformations for ground surfaces are negligibly small.

As part of the FEM analyses different load cases, representing changes in machine tool operating conditions, were adopted, which is shown for successive time steps in Fig. 6. The operating conditions were obtained by changing: the cutting force (F_s), the clamping forces F_{mo}, the roller pressure force F_{dr} and cutting force action angle k.

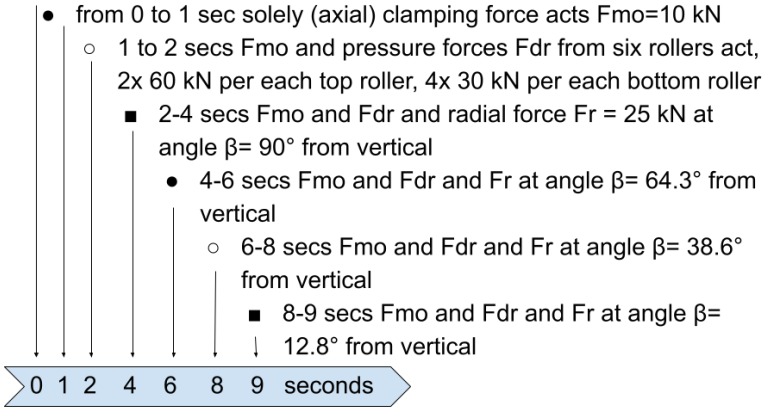

Fig. 6. Computation time steps and wheel set load cases in FEM computations; F_r – radial force, F_{mo} – clamping force, F_{dr} – roller pressure forces, β – radial force action angle

The whole loading cycle lasted 9 seconds. In the time interval from 0 to 1 sec solely clamping force F_{mo} equal to 10 kN, constituting the axial load, acted on the wheel set. In the next step, i.e. from 1 to 2 secs, besides the clamping force also roller pressure forces F_{dr} appeared. The loading system comprised six rollers – three per each wheel (Fig. 2). The top roller exerted the pressure of 60 kN while the two bottom rollers loaded the wheel with the force of 30 kN each. The load values are related to the machine specifications. In the 2-4 seconds interval besides the previously acting forces F_{mo} and F_{dr}, an additional cutting force amounting to 25 kN and acting radially was introduced. The force was situated at angle β = 90 degrees relative to the vertical. In the further part of the cycle the direction of cutting force action changed gradually. This angle amounted to β = 64.3°, β = 38.6° and β =12.8° in respectively the 4–6 secs interval, the 6–8 secs interval and the 8–9 secs interval.

3. IDENTIFICATION OF ERRORS CAUSED BY RADIAL DEFORMATIONS

The first to be determined were the causes of machining errors related to the elastic displacements of the wheel set. The wheel set was loaded with a radial force (F_r) at various angular positions β, as well as loads from the rollers (F_{dr}) and the longitudinal pressure of the wheel set F_{mo}. The radial displacements caused by the load generated by Fr were analysed at different amplitudes of this force – from the minimal value of 15000 N to the maximum value

of 27500 N (as in Fig. 9). Moreover, the effect of angular position β of the radial cutting force for β of 0–90° and factors relating to the mass and stiffness of the wheel structure were examined.

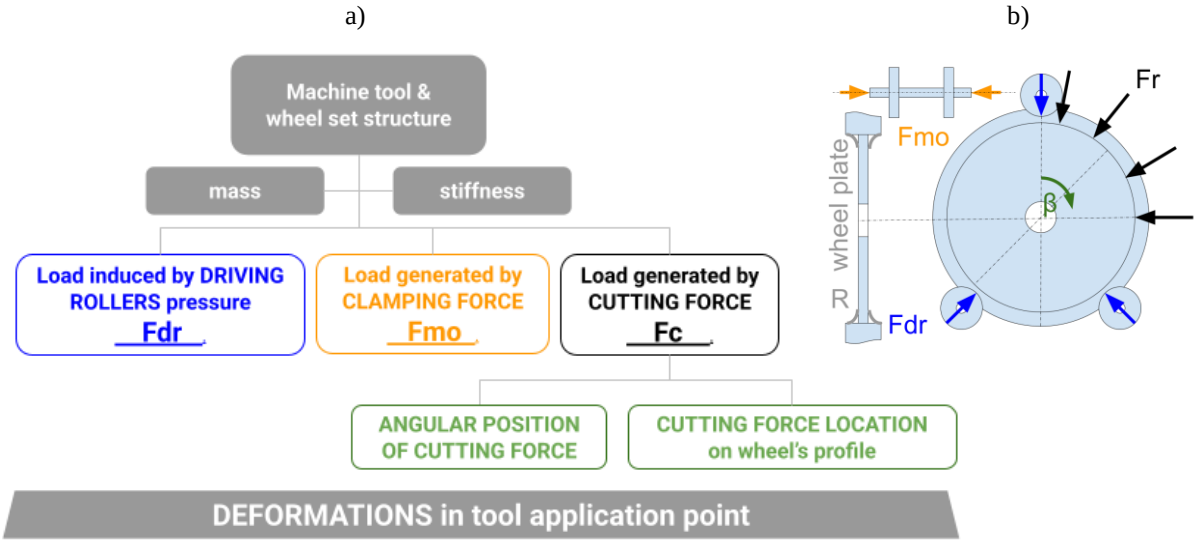

Fig. 7. a) Factors affecting wheel set radial displacements in tool application point, b) schematic of wheel with analysed factors, including structural changes in wheel plate, thickness and radii R

The wheel set's stiffness was changed through structure modifications consisting in adding casting radii R to the wheel and increasing the wheel's plate thickness from 21 mm to 84 mm (Fig. 7b). Figure 8 shows that the addition of casting radii results in a considerable increase in stiffness, corresponding to a quadruple increase in wheel plate thickness.

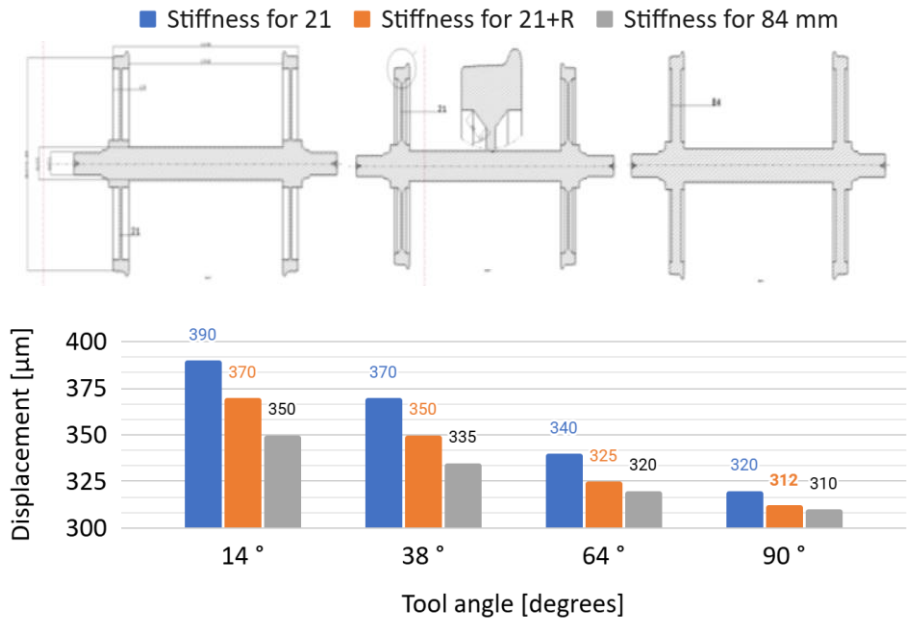

Fig. 8. Radial displacements in wheel sets with different stiffnesses (wheel plate thickness of 21 mm, 84 mm and 21 mm with radius R) at different cutting tool angles β = (14°, 38°, 64°, 90°)

As regards changes in the forces (F_{dr}) generated by driving rollers caused by their unbalance in the vertical direction or their wear, tool angle β = 90° ensures their minimal effect on machining precision. This is visible in Fig. 8 showing results for a wheel with different stiffnesses and loaded with a radial cutting force and forces originating from the driving rollers, resulting in radial deformations of 0-70 µm at tool angle β of 14–90°.

The stiffnesses of the machined wheels have the smallest effect on displacements at β = 90° (the red line and the yellow line in the diagram in Fig. 9b). This is confirmed in Fig. 8 which shows that the constant radial cutting force causes radial deformations in the place where it acts ranging from 310 to 380 µm at angle β of 90°–14°, respectively. Whereas in Figs 9a and 9b, where the radial cutting force ranges from 15000 to 27500 N at the angle of 14°, the displacements of the wheel set in the cutting point change from 300 to 360 µm, respectively.

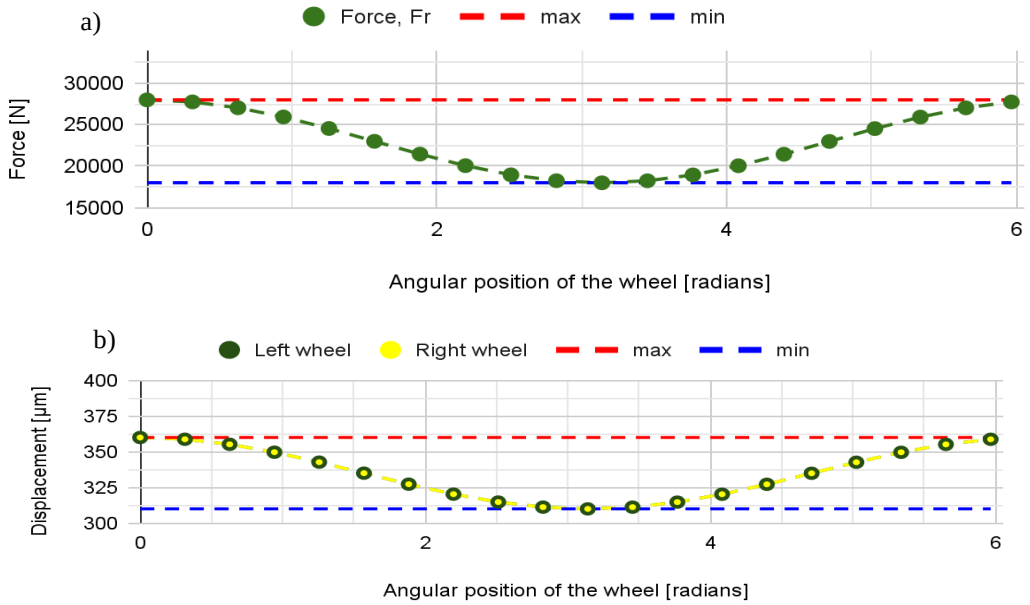

Fig. 9. Effect of changes in cutting forces on machining error for tool positioned at angle β = 14°; a) change in cutting force from min to max and corresponding b) radial displacements depending on wheel angular position

The following conclusions emerge from the FEM analysis of the errors:

- The deformations caused by a variable force leading to the loss of the machined wheel's circularity are highly complex due to the difficult to predict random character of the changes.
- The change of the forces from 15000 to 27500 N for the tool at angle β = 14° results in a 60 µm machining error.
- Tool position angle β = 90° ensures that the effect on machining accuracy is minimal.

4. IDENTIFICATION OF RADIAL AND AXIAL WHEEL PROFILE DEFORMATIONS

Limiting oneself to the radial force in the supervision and compensation of errors is fraught with major inaccuracies, particularly in the profile's rim area (profile points 3 to 7,

Fig. 10) where a large part of the deformation depends on axial force F_a. Therefore, further computations were carried out for the action of the radial cutting force (F_r) and the axial cutting force (F_a), forming an F_r/F_a ratio and applied to points 1–7 on the wheel's profile at angle $\beta = 14°$ used by the manufacturer.

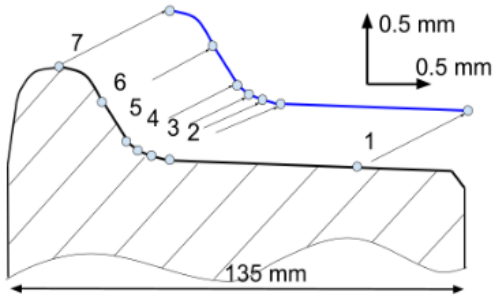

Fig. 10. Wheel profile after elastic deformations for F_r/F_a = 12500/12500 N. Nominal wheel profile with points 1 to 7 and profile after machining are marked with black line and blue line, respectively

Figure 11 shows the results of the computations of radial and axial displacements in the point of application of the tool for the left wheel and the right wheel.

The displacements of the left wheel's nominal profile are presented graphically in Fig. 10. The blue line represents the profile's elastic deformations caused by the action of the component cutting forces at their ratio F_r/F_a = 12500/12500 N in relation to the nominal profile marked with a black line. Moreover, the seven numbered points in which displacements resulting from tool action during machining were recorded are marked on the black profile.

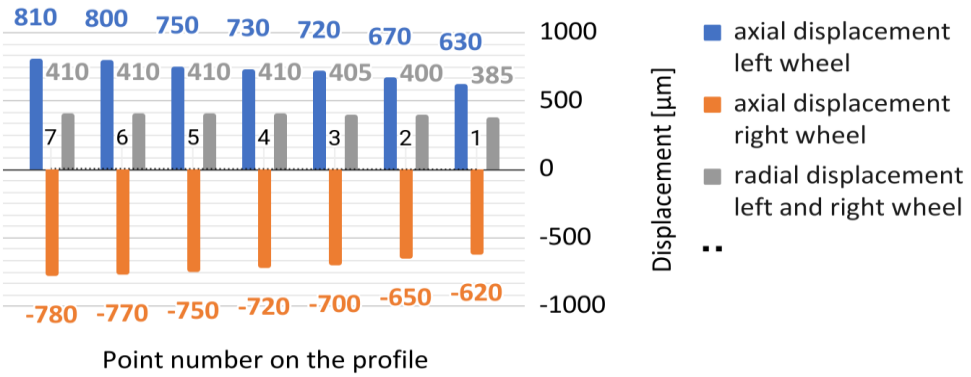

Fig. 11. Left and right wheel radial and axial displacement values in tool application point along profile for points 1–7 at F_r/F_a = 12500/12500

The radial and axial stiffness results, minimal and maximal from all the seven points, for different ratios F_r/F_a (radial force to axial force) are presented in Figs. 12a and 13b. It appears that the least stiff area is the profile's section from point 3 to 7, where the difference in radial stiffness between the min value and the max value is largest for different Fr/Fa ratios. For F_r/F_a = 12500/12500 (Fig.11) the axial displacement component significantly increases from 630 to 810 µm for the left wheel and from 620 to 780 µm for the right wheel, while radial displacement is almost constant (ranging from 405 to 410 µm).

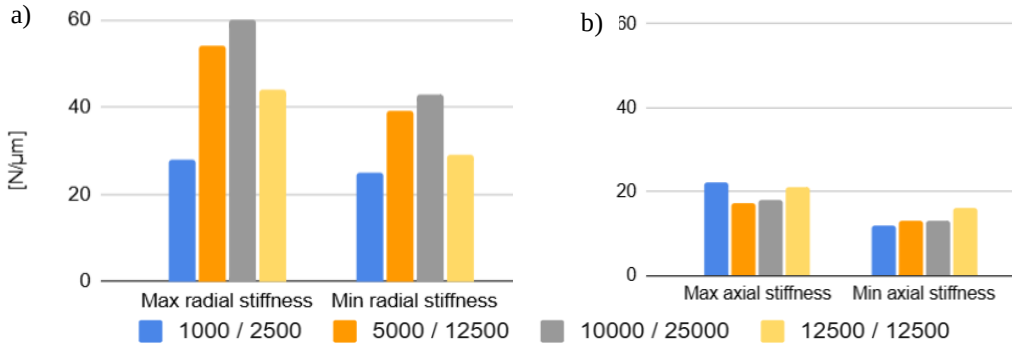

Fig. 12. Maximum and minimum: a) Wheel set's radial stiffness, b) axial stiffness, depending on radial force to axial force ratio (F_r/F_a)

Figure 12 clearly shows that radial stiffness is greater than axial stiffness and significantly depends on the radial/axial force ratio (F_r/F_a). It is not easy to determine the components of the cutting forces, the more so that they change rather quickly during machining. In order for online compensation to be effective the response to these changes must be quick. FEM analyses are useful for determining the forces and the displacements, but they are time-consuming. However, the data obtained as a result constitute a valuable source of information used to train AI tools. Thanks to such analyses one can prepare a set of data for various cases and use the data to train artificial neural networks. Only a trained ANN is able to effectively determine machining errors on the basis of the measured forces and the knowledge acquired from the FE model. Such a hybrid AI model for determining deformation as a function of the forces is a functional form of error mapping.

5. DEVELOPMENT AND TESTING OF FUNCTIONAL FORM OF ERRORS FOR THEIR EFFECTIVE COMPENSATION

A machining error function which will quickly respond to changes in the machining process is needed for error compensation. It was decided to use artificial neural networks for this purpose as they make it possible to quickly determine errors on the basis of the forces measured during machining. In order to build an ANN (e.g., in program Qnet or Python) one needs a training set based on the results of the FEM model. Another crucial step is assessing the network's performance on data outside the training set. The obtained research results indicate that, under real-world machine tool operating conditions, the network will be able to generate the precise error value necessary for effective compensation.

In order to prepare data for ANN training, FE discretization density along the wheel's profile within the wheel's rim was increased. Consequently, the number of points observed on the profile increased from 7 to 15.

Due to the complex dependence of stiffness on the force ratio F_r/R_a shown in Fig. 13, a training set was built with variable cutting force values for different force ratios F_r/F_a.

Considering the complex interrelation of stiffness on the force ratio F_r/R_a (shown in Fig. 12) a training set with variable cutting force values for various force ratios F_r/F_a was built. The first data set contained forces F_r/F_a =1/1 having values described by cases from P1 to P10. The cases are: P1 – 0/0, P2 – 3333/3333, P3 – 6666/6666, P4 – 10000/10000, P5 –

13333/13333, P6 – 16666/16666, P7 – 20000/20000, P8 – 23333/23333, P9 – 26666/26666, P10 – 30000N/30000N. The radial and axial displacement results for these forces in the consecutive profile points are presented in Fig. 12 and Fig. 13, respectively.

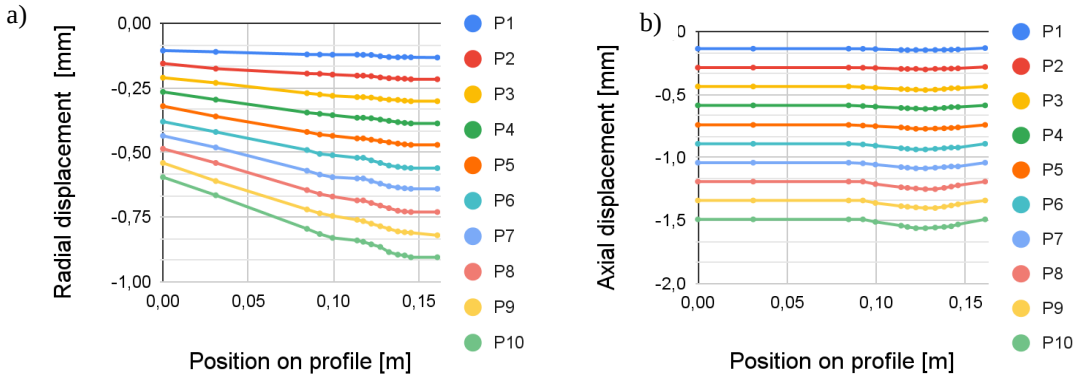

Fig. 13. Effect of forces F_r/F_a = 1/1 on: a) radial, b) axial displacements of wheel profile points. P1–P10 are different cases when forces F_r/F_a = 1/1

Similar computations of radial and axial displacements were performed for force ratios F_r/F_a =1/3, 2/3 and 1/2. For case 1/1 a diagram of the axial force and the radial force and the computed displacements depending on the profile point number are shown in Fig. 14.

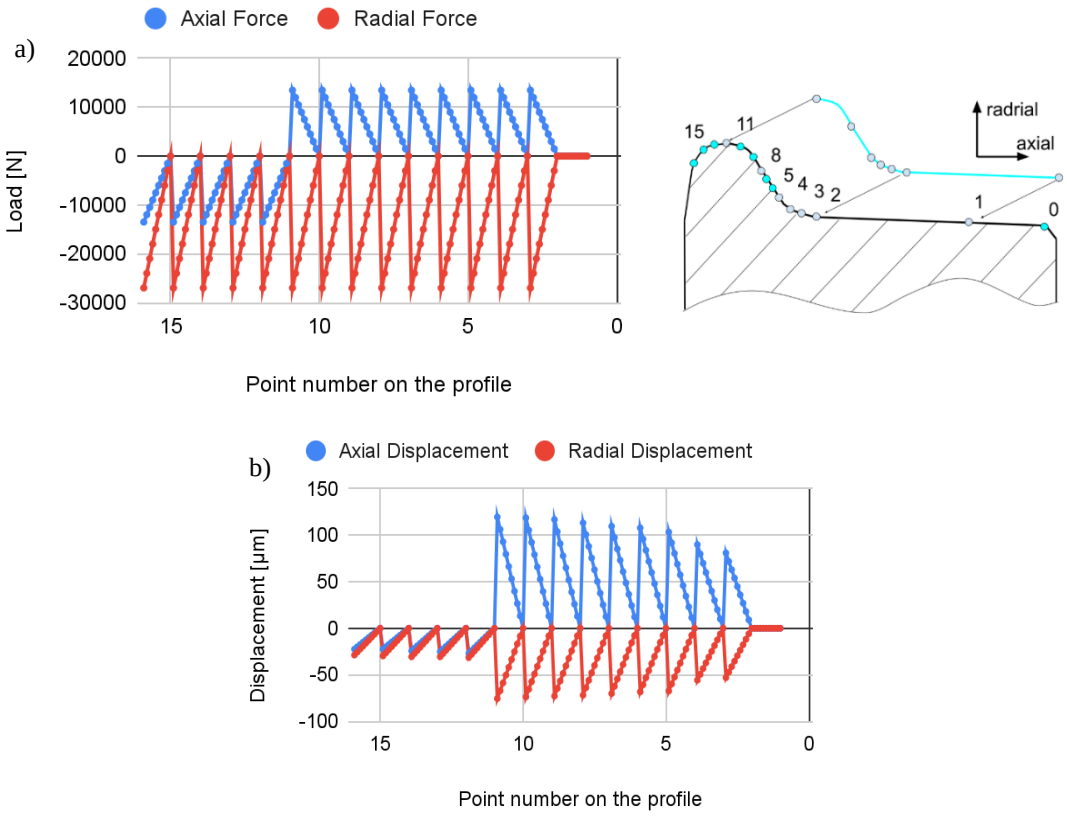

Fig. 14. Effect of radial force and axial force on radial and axial displacements of wheel profile points: a) force diagram for F_r/F_a=1/2 and b) corresponding displacements depending on profile point

The change in the sign of forces Fax in point 11 to 15 means that machining takes place on the wheel rim side which does not engage with the rail. In such a case a change in the direction of axial feed and in the direction of the action of force Fax is needed. The load in consecutive cutting force application points on the wheel's profile was analysed. In each point force values were changed 10 times from 0 N to F_{max} at proportions 1/1, 1/2, 1/3, obtaining corresponding displacement values in the force application points. In this way over 700 training cases were obtained.

For the data obtained for the wheel profile an artificial neural network was built for determining the radial and axial displacements on the basis of the position on the profile, the axial force and the radial force. The analysed profile and a diagram of the ANN are shown in Fig. 15.

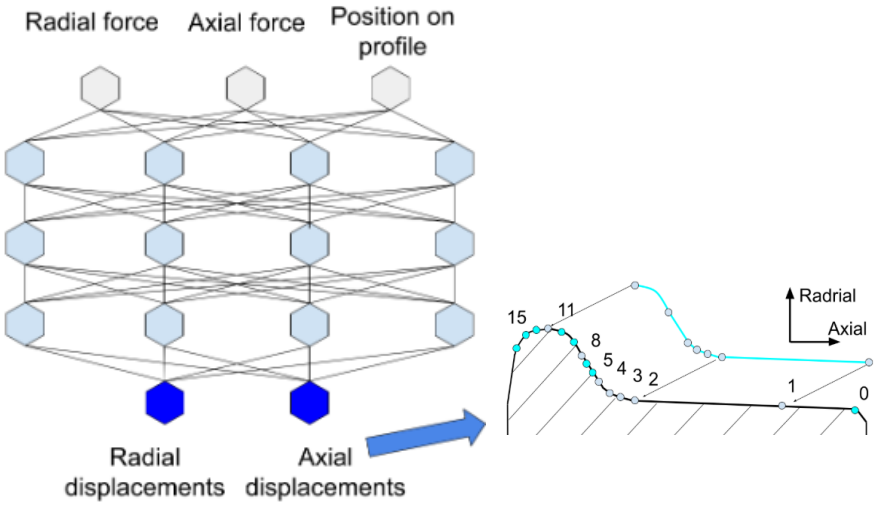

Fig. 15. Diagram of ANN used to determine displacements of points on selected part of profile

A simple five-layer ANN with a linear and sigmoid transfer function with inputs and outputs normalization was used. There were 681 training cases and 40 randomly selected testing cases.

Initially the functioning of the ANN was tested for all the profile points and the following were obtained for the training data:

- output 1, p-rad, Std_Dev = 4.41 μm, max error= 23.5 μm, correlation = 0.9998;
- output 2, p-ax; Std_Dev = 15.03 μm, max error= 87.4 μm; correlation = 0.9996.

The following were obtained for the testing data:

- output 1, p-rad, Std_Dev = 3.61 μm, max error= 12.5 μm, correlation = 0.9999;
- output 2, p-ax, Std_Dev = 21.39 μm, max error= 87.1 μm, correlation = 0.9993.

In order to improve ANN learning accuracy, training was limited to selected points on the profile, i.e. the ones on the side where it engages with the rail. The reason for this is that machining quality is determined by the precision with which this part of the profile is machined.

The following were obtained for the limited profile for the training data:

- output 1, p-rad, Std_Dev = 2.46 μm, max error= 8.16 μm, correlation = 0.9999,
- output 2, p-ax; Std_Dev = 9.27 μm, max error= 32.4 μm, correlation= 0.9998.

The following were obtained for the testing data:

- output 1, p-rad, Std_Dev= 2.44 µm, max error= 50.0 µm, correlation=0.9999;
- output 2, p-ax, Std_Dev= 7.92 µm, max error= 16.5 µm, correlation= 0.9998.

A double improvement in the modelling of elastic deformations along both the radial and axial deformation directions was obtained for the training data.

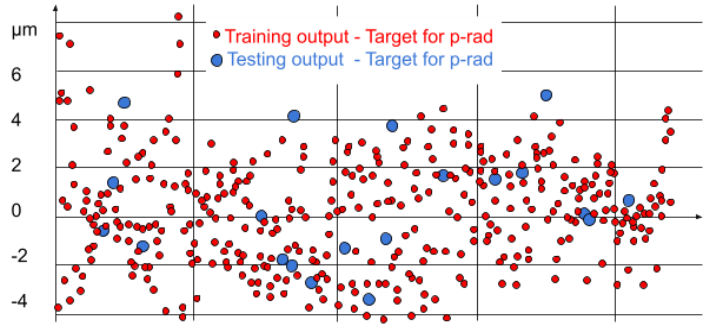

Fig. 16. Difference between p-rad ANN output for training and testing data and target value

The value of correlation for both the training set and the testing set for both directions of displacements is close to 1. The standard deviation (Std) for the two sets reached values from 2.5 to 9 µm. Figure 16 shows the distribution of errors in the adopted ANN training and testing space. The points represent the difference between the value at the ANN's output (p rad) and the target value. The red points are for training data while the blue ones are for the testing data.

6. TESTING ANN ON DATA SET NOT USED TO TRAIN IT

Since in a real case it is difficult to determine the proportions of the forces acting on the wheel set, a set of testing forces at different ratios was defined. The set of testing forces consists of four consecutive cases in which the cutting force's axial component and radial component take part. The variability of their ratio was obtained by changing the radial force from 0 to 30000 N for each axial component having the value of 5000, 10000, 20000 and 30000 N. The amplitude of the radial force would change at every 0.1 sec as shown in Fig. 17. For this set of forces displacements were calculated using the FE model (Fig. 18a). The FEM calculation results for the above data were compared with the results yielded by the ANN trained on the data set presented in Section 5.

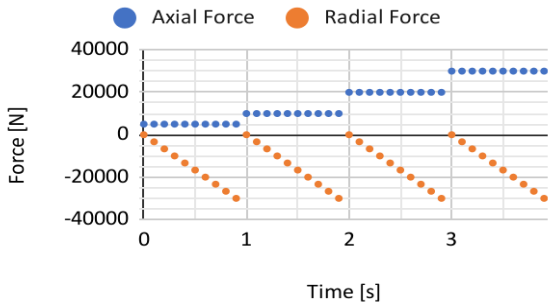

Fig. 17. Set of testing forces used to load wheel set

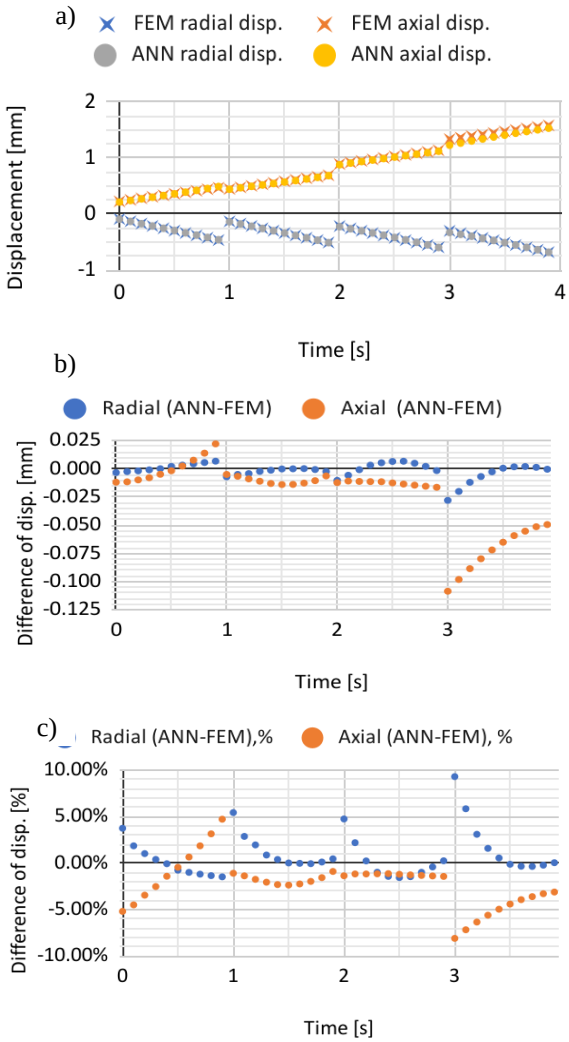

Fig. 18. Comparison of ANN results with FEM results for testing data not used to train ANN: a) displacement results, b) difference displacement between ANN and FEM, c) percentage difference displacement between ANN and FEM relative to FEM calculated value

For the second set of cases (Fig. 17.) a small difference between the results yielded by the FEM analysis and the responses obtained from the previously trained ANN was found (Fig. 18a). Figure 18b shows that the largest difference does not exceed 0.110 mm and 0.050 mm for respectively axial and radial displacements. These differences in relation to the total displacements yielded by FEM do not exceed 10% (Fig. 18c), which is a satisfactory result. This is evidence of the high usefulness of artificial neural networks for predicting the deformations of a train wheel set during its machining.

7. CONCLUSION

A precise numerical model for evaluating machining errors and analysing the behaviour of a train wheel set in various conditions of turning on specialized machine tools for reconditioning and shaping the profile of train wheels has been developed. As part of FEM

investigations comprehensive qualitative research for selected computing mesh parameters, boundary conditions and way of modelling the bearings was carried out ensuring high reliability of the mapping of the actual phenomena. It was shown that wheel set type and wheel geometry have a decisive effect on the wheel's stiffness, particularly in the profile rim area which is characterized by the lowest resistance to deformation.

On the basis of the set of data generated by the FE model an artificial neural network was built. Its functioning and usefulness were verified on the model developed for determining elastic deformations in the radial and axial directions, arising as a result of the action of cutting forces. The obtained results constitute a basis for developing a sensoric-parametric machining error compensation method which uses the measurement of cutting forces and the error values determined by an ANN for error corrections in the machine tool's control axes.

Analyses of the effect of radial and axial forces showed that machining precision depends on the values of the forces and the angle of the tool position on the circumference of the wheel. The force amplitude variation from 15000 to 27500 N for a tool at an angle of β = 14° causes a machining error of 60 μm. Positioning the tool at β = 90° minimizes the effect the wheel set's stiffness on displacements.

Thanks to the use of artificial neural networks it became possible to effectively map the nonlinear force-deformation dependences and obtain high agreement between the ANN results and the results of FEM analyses. This confirms the high usefulness of the AI approach in predicting the mechanical behaviour of train wheel sets, whereby machining errors in specialized machine tools can be effectively compensated.

Restricting the modelling to selected points of the profile resulted in a significant, approximately twofold improvement in the accuracy of the neural network predictions for both the training and testing datasets. For the radial direction, the standard deviation of error decreased from about 4.4 μm to 2.5 μm (training) and from 3.6 μm to 2.4 μm (testing), while for the axial direction it decreased from about 15 μm to 9 μm (training) and from 21 μm to 8 μm (testing). At the same time, correlation coefficients remained very high ($\geq$ 0.9998). These results confirm that selecting specific profile points reduced modelling errors by 40–60%, leading to more than a twofold improvement in the accuracy of elastic deformation modelling in both radial and axial directions.

Further research on the ANN for effective error compensation will involve:

- adding inputs to the ANN in order to incorporate the wheel set's design parameters,
- the evaluation of the correlation between the actual behaviour of the wheel set and the values used to train the ANN.

ACKNOWLEDGEMENTS

The author would like to thank Zbigniew Kowal, PhD for carrying out the analyses and for his valuable comments made during the preparation of this paper, which helped to improve its quality. The research was carried out as part of the INTOR, POIR.04.01.04-00-0067/17-00 project in the years 01.06.2018 – 31.05.2021, co-funded by NCBiR (The National Centre for Research and Development https://www.gov.pl/web/ncbr-en) Created using resources provided by Wroclaw Centre for Networking and Supercomputing (http://wcss.pl).

DEDICATION

This paper is dedicated to the memory of Prof. Jerzy Jedrzejewski, DSc, Eng. on behalf of the whole research team. His vision, support and commitment were invaluable for the realization of the research which became the basis for this publication.

REFERENCES

[1] SHOKRANI A., DOGAN H., BURIAN D., NWABUEZE T.D., KOLAR P., LIAO Z., SADEK A., TETI R., WANG P., PAVEL R., SCHMITZ T., 2024, *Sensors for In-Process and on-Machine Monitoring of Machining Operations*, CIRP Journal of Manufacturing Science and Technology, 51, 263–292.

[2] WU L., WANG A., WANG K., XING W., XU B., ZHANG J., YU Y., 2024, *Adaptive Optimization Method for Prediction and Compensation of Thin-Walled Parts Machining Deformation Based on On-Machine Measurement*, Sensors, 24/2, 613.

[3] LI Y., CHENG X., ZHENG G., YAN J., LIU H., LI X., 2022, *Dynamic Modeling and In-Process Parametric Compensation for Fabricating Micro Straight Thin Walls by Micromilling*, Journal of Materials Research and Technology, 18, 2480–2493.

[4] GE G., DU Z., FENG X., YANG J., 2020, *An Integrated Error Compensation Method Based on on-Machine Measurement for Thin Web Parts Machining*, Precision Engineering, 63, 206-213.

[5] NAUMANN C., NAUMANN A., BERTAGGIA N., GEIST A., GLÄNZEL J., HERZOG R., ZONTAR D., BRECHER CH. DIX M., 2023, *Hybrid Thermal Error Compensation Combining Integrated Deformation Sensor and Regression Analysis Based Models for Complex Machine Tool Designs*, International Conference on Thermal Issues in Machine Tools (ICTIMT2023), Cham: Springer International Publishing, 28–40.

[6] GENG Z., TONG Z., JIANG X., 2021, *Review of Geometric Error Measurement and Compensation Techniques for Machine Tools*, Light: Advanced Manufacturing, 2/2, 211–227.

[7] DENKENA B., DAHLMANN D., PETERS R., WITT M., 2017, *Model Based Compensation of Geometrical Deviations Due to Process Forces*, Journal of Machine Engineering, 17/1, 5–16.

[8] BRECHER C., WETZEL A., BERNERS T., EPPLE A., 2019, *Increasing Productivity of Cutting Processes by Real-Time Compensation of Tool Deflection Due to Process Forces*, Journal of Machine Engineering, 19/1, 16–27.

[9] PIORKOWSKI P., SKOCZYNSKI W., 2021, *Evaluation of Milling Machine Properties Based on Shape Errors*, Advances in Science and Technology Research Journal, 15/2, 148–155.

[10] LEI M., YANG J., WANG S., ZHAO L., XIA P., JIANG G., MEI X., 2019, *Semi-Supervised Modeling and Compensation for the Thermal Error of Precision Feed Axes*, The International Journal of Advanced Manufacturing Technology, 104, 4629–4640.

[11] KOWAL Z., JEDRZEJEWSKI J., GIM T., 2020, *Precision of Prestressed Ball Screw Thermal Behaviour in Machine Tool Operating Conditions*, Int. J. Nanomanufacturing, 16/1, 29–39, https://doi.org/10.1504/IJNM.2020.104478

[12] JEDRZEJEWSKI J., KOWAL Z., KWASNY W., WINIARSKI W., 2014, *In-House System for Holistic Modelling of Machine Tool Operating Properties*, 2nd International Conference on Systems and Informatics (ICSAI 2014), IEEE, 15–17.

[13] PN-EN 13715:2020-12 *Railway applications -- Wheelsets and bogies -- Wheels -- Tread profile*.

[14] MACIOLKA P., JEDRZEJEWSKI J., KWASNY W., 2022, *Evaluation of the Reliability of Contact Characteristic Simulation Results by The Experimental-Computational Method*, Tribology International, 165, 107335, 1–7, https://doi.org/10.1016/j.triboint.2021.107335.